# On the Compressive Heating/Cooling Mechanism in Thermal Elastohydrodynamic Lubricated Contacts

W. Habchi[*1] and P. Vergne[2]

[1] Lebanese American University, Department of Industrial and Mechanical Engineering, Byblos, Lebanon
[2] Université de Lyon, INSA-Lyon, CNRS, LaMCoS UMR5259, F-69621, France

*Corresponding author: wassim.habchi@lau.edu.lb

**Abstract**

The importance of compressive heating/cooling occurring within lubricating films in thermal elastohydrodynamic lubricated contacts has not been given sufficient attention in the literature. This paper presents a numerical investigation of this mechanism and attempts to quantify its importance as compared to shear heating under pure-rolling and rolling-sliding conditions. It is found that even under pure-rolling, compressive heating/cooling remains in most cases less important than shear heating or at best, of the same order. Under rolling-sliding conditions, as soon as the slightest sliding occurs, heat generation is governed by shear heating. The dependence of compressive heating/cooling on operating conditions is also examined. Finally, the impact of this mechanism on the lubricating performance of these contacts is considered under various operating conditions.

**Keywords:** Elastohydrodynamic Lubrication; Compressive Heating/Cooling; Thermal Effects; Finite Elements;

## 1. Introduction

Heat generation within lubricating films of elastohydrodynamic lubricated (EHL) contacts can be a consequence of two separate mechanisms: lubricant compression/decompression and lubricant shear. The former is a consequence of a pressure build-up at the inlet of EHL contacts which leads to a compression of the lubricant accompanied by a generation of heat. But, at the exit of the contact, the pressure drop is associated to a decompression of the lubricant leading to the formation of a "heat sink" within the lubricating film. This combined heating/cooling mechanism by lubricant compression/decompression is often referred to as "compressive heating/cooling effect". On the other hand, shear heating is a consequence of lubricant layers moving at different speeds and rubbing against each other across the lubricant film thickness, leading to frictional heat generation (shear heating). This is most pronounced under rolling-sliding or pure-sliding conditions where surface velocities of the contacting elements are

different, but can also occur under pure-rolling conditions. In fact, under pure-rolling conditions, though the “Couette” component of the lubricant flow leads to a constant velocity distribution across the lubricant film thickness due to identical surface velocities of the contacting elements, the velocity profile itself is not constant, owing to the pressure-driven “Poiseuille” component of the flow [1]. This results in neighboring lubricant layers rubbing against each other and generating heat.

The interest in EHL thermal effects first appeared with the pioneering theoretical work of Cheng [2] [3]. The first full numerical solution for the point contact problem was obtained by Zhu and Wen [4]. Since then, several authors proposed different methods to deal with this problem assuming a Newtonian or a non-Newtonian lubricant such as Kim and Sadeghi [5], Guo et al. [6] , Kaneta et al. [7] or also Liu et al. [8] who solved the three-dimensional energy equation in order to determine the temperature variations throughout the lubricant film. An alternative method consists in reducing the three-dimensional heat transfer problem to a two-dimensional one by assuming a parabolic temperature distribution across the film thickness. This approach was used by many researchers; however, the parabolic temperature profile simplification leads to temperature predictions that are not accurate especially at the inlet of the contact as shown by Kazama et al. [9]. The reason lies in the occurrence of complex thermal convective effects which are associated with important reverse flows in this area. Salehizadeh and Saka [10] highlighted in their thermal non-Newtonian analysis of line contacts the importance of compressive heating in raising the lubricant’s temperature in the inlet of the contact. Surprisingly, Kaneta et al. [11] found that compressive heating had an important impact on friction in EHL contacts at low levels of sliding (this issue will be discussed in further detail at a later stage). Sadeghi and co-authors [12] [13] carried out a numerical analysis of thermal newtonian EHL point contacts and investigated the effect of compressive heating/cooling on temperature under pure-rolling conditions. They found that temperature increases in the inlet area due to shear heating and rises further more due to compressive heating but then falls in the exit region of the contact because of decompression cooling. They predicted a maximum temperature rise of about $10^{o}$C and also found that in the presence of sliding the thermal response of the contact was governed by shear heating. In the experimental study of Reddyhoff et al. [14], the authors used an infrared temperature mapping technique with a ball-on-disk test-rig to investigate the effects of compressive heating/cooling on temperature rise in EHL contacts. Their tests were carried out both in “nominally pure-rolling”**,** with the disc driving the ball, and in “forced pure-rolling” with the ball and disc being driven at the same surface speed using separate motors. However, being a work of experimental nature, the authors had very little access to what is actually happening within the lubricant film at the local level, so they could not really quantify the share of compressive heating/cooling in their temperature rise measurements as compared to that of shear heating.

From the earliest works listed above, it was recognized that heat generation within EHL conjunctions is a consequence of both lubricant compression and lubricant shear and both aspects were taken into consideration in the solution of the thermal part of the problem.

Furthermore, most of these works acknowledge that the compressive/heating cooling effect is only significant under pure-rolling conditions and that, whenever sliding occurs, this effect becomes negligible compared to shear heating. However, none of these has examined this issue in more detail in an attempt to quantify the importance of compressive heating/cooling compared to shear heating and under which conditions the former became negligible compared to the latter. The current work provides a numerical investigation of compressive heating/cooling in EHL circular contacts. The advantage of a numerical approach (as compared to an experimental one such as that of Reddyhoff et al. [14]) is that the actual impact of compressive/heating cooling on lubrication performance may be quantified by simply switching this effect off and then back on in the numerical simulations; something that cannot be done in an experimental setup. In addition, the importance of compressive heating/cooling as compared to shear heating may also be exactly quantified under different operating conditions. The employed numerical model is the full-system finite element approach for the solution of the thermal EHL problem [15] [16] introduced by the authors in recent years. This approach has been successfully used in predicting the lubricating performance of EHL contacts in terms of film thickness [15] as well as friction [17]. By "successfully" it is meant that a thorough validation against experiments has been attained. In this work, only circular contacts will be considered, however the findings and analysis are of a more general scope and may be extended to line or elliptical contacts. The outline of this paper is as follows: section 2 provides a description of the selected lubricant and the dependence of its rheological and transport properties on pressure, temperature and shear stress. Then in section 3, the main features of the employed numerical model are briefly recalled. Section 4.1 provides a quantification of compressive heating/cooling as well as shear heating and, most importantly, a magnitude comparison of these two effects within EHL contacts under a wide range of operating conditions under both pure-rolling and rolling-sliding regimes. In section 4.2, the impact of compressive heating/cooling on the lubrication performance of circular EHL contacts is quantified and finally a general conclusion is offered in section 5.

## 2. Selected Lubricant and its Properties

The lubricant selected for this work is a typical mineral oil (Shell T9) for which the rheological and transport properties have been thoroughly characterized in [17]. The variations of these properties with pressure, temperature and shear stress were measured and appropriate models were derived to represent these variations. The derived models are briefly recalled in the following. Subscripts *0* and *R* indicate, respectively, ambient conditions and a reference state which are taken to be the same in the current work ( $p_0 = p_R = 0$ and $T_0 = T_R = 25^o\mathrm{C}$ ). The Murnaghan [18] equation of state is used to model the density variations with pressure *p* and temperature *T*:

$$\rho = \frac{\rho_R}{1+a_V\left(T-T_R\right)} \times \left(1+\frac{K_0'}{K_0}p\right)^{\frac{1}{K_0'}} \quad \text{with} \quad K_0 = K_{00}\exp\left(-\beta_K T\right) \qquad (1)$$

Where $K_0' = 10.545$, $a_V = 7.734\times10^{-4}\ \mathrm{K}^{-1}$, $K_{00} = 9.234\ \mathrm{GPa}$, $\rho_R = 875\,Kg/m^3$ and $\beta_K = 6.090\times10^{-3}\ \mathrm{K}^{-1}$ were obtained from experimental measurements. As for the viscosity dependence on temperature and pressure, a different and enhanced model is employed. In fact, in the current work, the improved Yasutomi correlation is used as proposed in [19]:

$$\mu = \mu_g \exp\left[\frac{-2.303\,C_1\left(T-T_g\right)F}{C_2+\left(T-T_g\right)F}\right] \qquad (2)$$

$$\text{with:}\quad T_g = T_{g0} + A_1\ln\left(1+A_2 p\right) \quad \text{and} \quad F = \left(1+B_1 p\right)^{B_2}$$

Where $A_1 = 188.86\ ^\circ C$, $A_2 = 0.719\ \mathrm{GPa}^{-1}$, $B_1 = 8.2\ \mathrm{GPa}^{-1}$, $B_2 = -0.5278$, $C_1 = 16.09$, $C_2 = 17.38^\circ C$, $T_{g0} = -83.2^\circ C$ and $\mu_g = 10^{12}\,Pa\cdot s$. As for the shear dependence of viscosity, the single-Newtonian modified Carreau-Yasuda equation [20] is used to define the generalized viscosity $\eta$ as a function of shear stress $\tau$ as follows:

$$\eta = \frac{\mu}{\left[1+\left(\frac{\tau}{G}\right)^a\right]^{\frac{\frac{1}{n}-1}{a}}} \qquad (3)$$

Where $G = 7.0\ \mathrm{MPa}$, $a = 5$ and $n = 0.35$. The lubricant was shown to exhibit a limiting shear stress behavior under high shear rates. The limiting value of the shear stress $\tau_L$ was shown to vary linearly with pressure according to the following relationship:

$$\tau_L = \Lambda\ p \qquad (4)$$

Where the limiting-stress pressure coefficient $\Lambda = 0.083$. Finally, the dependence of the thermal properties of this lubricant on pressure and temperature is considered. First, its thermal conductivity $k$ depends on temperature and pressure according to the following equation:

$$k = B_k + C_k\kappa^{-s} \qquad \text{with} \qquad \kappa = \left(\frac{V}{V_R}\right)\left[1+A\left(\frac{T}{T_R}\right)\left(\frac{V}{V_R}\right)^3\right] \qquad (5)$$

Where $A = -0.101$, $B_k = 0.053\ \mathrm{W/m\cdot K}$, $C_k = 0.026\ \mathrm{W/m\cdot K}$, $s = 7.6$ and the term $V/V_R$ is nothing else but $\rho_R/\rho$ obtained directly from equation (1). As for the volumetric heat capacity $C = \rho c$ of this lubricant, it depends on temperature and pressure as follows:

$$C = C' + m\chi \qquad \text{with} \qquad \chi = \left(\frac{T}{T_R}\right)\left(\frac{V}{V_R}\right)^{-4} \qquad (6)$$

Where $C' = 1.17\times10^{6}\ J/m^{3}\cdot K$, $m = 0.39\times10^{6}\ \mathrm{J/m^{3}\cdot K}$ and the term $V/V_R$ is obtained from equation (1). It is noteworthy to mention that the above rheological models were derived from actual measured transport properties and used without any alteration of their corresponding parameters to predict film thickness and friction in EHL circular contacts under a wide range of operating conditions [17]. The predicted results showed excellent agreement with experiments, allowing the authors to establish a validated framework for the theoretical prediction of the lubricating performance of EHL contacts. The employed rheological models are (compared to the ones commonly used in the EHL literature) relatively complex with multiple parameters to be determined from experiments. However, the importance of using such relations that are derived from a sound physical background for an accurate prediction of the lubricating performance of EHL contacts has been thoroughly discussed in [17] [21] [22]. Next, the numerical model employed in this work is briefly recalled.

## 3. Numerical Model Description

The numerical model employed in this work is based on the full-system finite element approach developed in recent years by the authors and described in detail in [15] [16]. Here, only its main features are recalled. In section 3.1, the EHL part is described and its corresponding equations recalled. The thermal part is described in section 3.2 and finally, the overall numerical procedure is recalled in section 3.3.

### 3.1. EHL Part

The EHL part of the model consists of three main equations: the generalized Reynolds applied to the 2D contact area $\Omega_c$ (see figure 1 (a)); the linear elasticity equations applied to the 3D solid domain and the load balance equation. The Reynolds equation for a steady-state point contact between a sphere and a flat plane lubricated with a generalized Newtonian lubricant under unidirectional surface velocities in the x-direction is given by Yang and Wen [23]:

$$\frac{\partial}{\partial x}\left[\left(\frac{\rho}{\eta}\right)_e h^3 \frac{\partial p}{\partial x}\right] + \frac{\partial}{\partial y}\left[\left(\frac{\rho}{\eta}\right)_e h^3 \frac{\partial p}{\partial y}\right] = 12\frac{\partial}{\partial x}\left(\rho^* U_m h\right) \qquad (7)$$

$$U_m = \frac{u_p + u_s}{2} \qquad \left(\frac{\rho}{\eta}\right)_e = 12\left(\frac{\eta_e \rho'_e}{\eta'_e} - \rho''_e\right)$$

Where:
$$\rho^* = \frac{\left[\rho'_e \eta_e \left(u_s - u_p\right) + \rho_e u_p\right]}{U_m} \qquad \rho_e = \frac{1}{h}\int_0^h \rho\, dz$$

$$\rho'_e = \frac{1}{h^2}\int_0^h \rho \int_0^z \frac{dz'}{\eta} dz \qquad \rho''_e = \frac{1}{h^3}\int_0^h \rho \int_0^z \frac{z' dz'}{\eta} dz$$

$$\frac{1}{\eta_e} = \frac{1}{h}\int_0^h \frac{dz}{\eta} \qquad \frac{1}{\eta'_e} = \frac{1}{h^2}\int_0^h \frac{z\, dz}{\eta}$$

Indices *p* and *s* correspond to the plane and the sphere respectively and the film thickness *h* in equation (7) is replaced by:

$$h(x,y) = h_0 + \frac{x^2 + y^2}{2R} - \delta(x,y) \qquad (8)$$

Where *R* is the radius of the ball and *δ(x,y)* corresponds to the normal elastic deformation of the solid surfaces at a given point (x,y) of the 2D contact area $\Omega_c$. Note that, under the range of operating conditions considered in this work, thin-film assumptions and the use of the generalized Reynolds equation are entirely justified and pressure variations across the film thickness should be negligible. Only the velocity profile might be inaccurate in the inlet region of the contact, as reported in CFD simulations of EHL contacts (see for instance [24]). But this has no influence on compressive heating. The normal elastic deformation of the solid surfaces is obtained by solving the linear elasticity equations on a large *3D* solid body representing a half-space domain as shown in figure 1 (a).

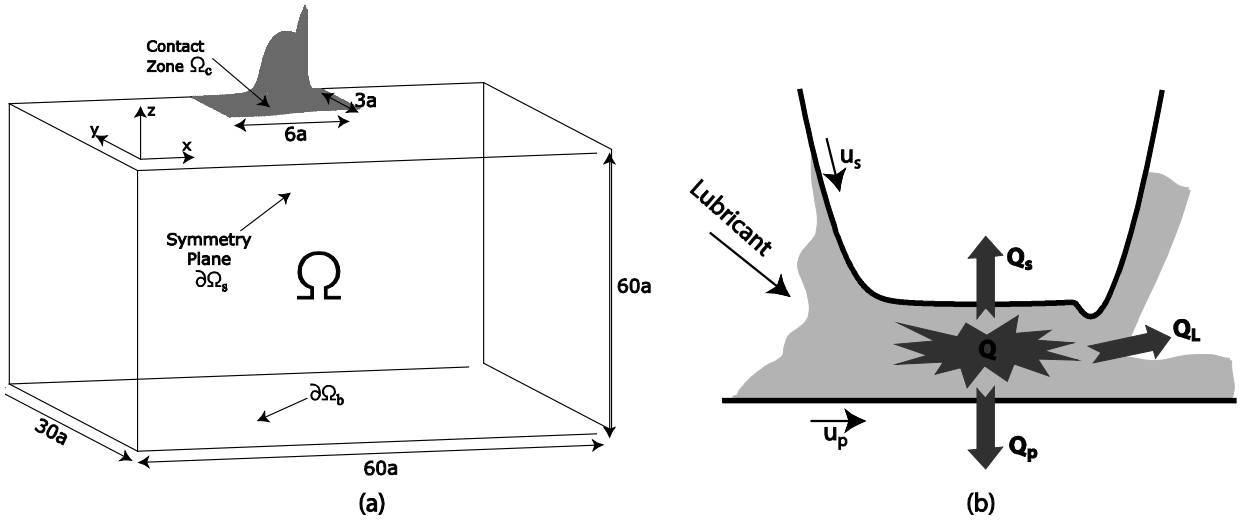


**Figure 1:** Geometrical domain of the EHL part (left) and overall geometry of the contact with associated heat transfer mechanisms (right)

Finally, the load balance equation is used to complete the EHL part of the model:

$$\int_{\Omega_c} p \, d\Omega = F \qquad (9)$$

This equation is used to ensure that the correct external load $F$ is applied to the contact by monitoring the value of the rigid body displacement $h_0$. The generalized Reynolds equation defined above is associated with the usual EHL boundary conditions. That is, zero pressure is assumed on the boundary of the contact area $\Omega_c$ and the free boundary problem arising at the exit of the contact is handled by applying a penalty method as proposed by Wu [25]. As for the linear elasticity part, the pressure distribution obtained from the Reynolds equation is used as a normal pressure load boundary condition on the contact surface $\Omega_c$ while a zero displacement boundary condition is applied on the bottom side $\partial\Omega_b$ of the 3D geometrical domain $\Omega$ at a sufficient distance from the contact area to approximate a half-space configuration. Finally, a zero normal stress boundary condition is applied to the rest of the boundaries of $\Omega$. The symmetry of the problem with respect to the *xz*-plane is taken into consideration to reduce its associated computational cost. For more details the reader is referred to [16].

### 3.2. Thermal Part

Heat is generated within the lubricant film by compression and shear as indicated earlier. Parts of the generated heat ($Q_s$ and $Q_p$) are dissipated towards the solids by conduction as shown in figure 1 (b). The solids then carry part of this received heat towards the contact exit by advection. Another part of the generated heat ($Q_L$) is carried out by the lubricant towards the exit of the contact by advection while some of the heat remains confined within the lubricant film leading to a local increase in its temperature. Heat transfer by conduction is dictated by the thermal conductivities of the solids and lubricant whereas advection is governed by their volumetric heat capacities and speeds. Temperature distribution in the two solid bodies and the lubricant film is obtained by solving the *3D* energy equation applied to their respective geometrical domains. For the solid parts *p* and *s* this equation reads:

$$\begin{cases} -k_p\left(\dfrac{\partial^2 T}{\partial x^2}+\dfrac{\partial^2 T}{\partial y^2}+\dfrac{\partial^2 T}{\partial z^2}\right)+\rho_p c_p u_p \dfrac{\partial T}{\partial x}=0 \\ -k_s\left(\dfrac{\partial^2 T}{\partial x^2}+\dfrac{\partial^2 T}{\partial y^2}+\dfrac{\partial^2 T}{\partial z^2}\right)+\rho_s c_s u_s \dfrac{\partial T}{\partial x}=0 \end{cases} \qquad (10)$$

As for the lubricant film, the same equation applies with the addition of the heat generation terms by compression ($Q_{comp}$) and shear ($Q_{shear}$):

$$-k\frac{\partial^2 T}{\partial z^2}+\rho c\left(u_f \frac{\partial T}{\partial x}+v_f \frac{\partial T}{\partial y}\right)=Q_{comp}+Q_{shear} \qquad (11)$$

With: $Q_{comp} = -\frac{T}{\rho}\frac{\partial \rho}{\partial T}\left(u_f \frac{\partial p}{\partial x} + v_f \frac{\partial p}{\partial y}\right)$ and $Q_{shear} = \eta\left[\left(\frac{\partial u_f}{\partial z}\right)^2 + \left(\frac{\partial v_f}{\partial z}\right)^2\right]$

Note that the heat generation terms $Q_{comp}$ and $Q_{shear}$ correspond to the power generated within the lubricant film per unit volume by compression and shear respectively. Also note that heat convection in the film thickness (*z*-direction) and heat conduction in the film plane (*xy*-plane) are neglected compared to convection in the film plane and conduction through the film thickness as proposed by most TEHL models in the literature (see for example references [3] and [6]). This is a consequence of the small dimension of the lubricant film in the *z*-direction as compared to the *x* and *y*-directions. The lubricant velocity field components $u_f$ and $v_f$ in the *x* and *y* directions respectively are given by:

$$\begin{aligned} u_f &= u_p + \frac{\partial p}{\partial x}\left[\int_0^z \frac{z'dz'}{\eta} - \frac{\eta_e}{\eta'_e} h \int_0^z \frac{dz'}{\eta}\right] + \frac{\eta_e\left(u_s - u_p\right)}{h}\int_0^z \frac{dz'}{\eta} \\ v_f &= \frac{\partial p}{\partial y}\left[\int_0^z \frac{z'dz'}{\eta} - \frac{\eta_e}{\eta'_e} h \int_0^z \frac{dz'}{\eta}\right] \end{aligned} \qquad (12)$$

Note that, as mentioned earlier, even under pure-rolling conditions ($u_p = u_s$), the lubricant velocity profile across the film thickness defined by ($u_f, v_f$) is not constant. In fact, both $u_f$ and $v_f$ vary in the z-direction through the integral terms found in equation (12) leading to heat generation by shear, even under pure-rolling conditions. Finally, for the boundary conditions of the thermal problem, an ambient temperature $T_0$ is applied at the inlet of the solid bodies and that of the lubricant film. Continuity of heat flux as well as temperature is imposed across the two lubricant-solid interfaces. The symmetry of the thermal part with respect to the *xz*-plane is also taken into consideration.

### 3.3. Overall Numerical Procedure

Equations (7-12) completely define the thermal EHL circular contact problem. All equations are discretized using a finite element approximation and solved in dimensionless form. The global numerical procedure consists in starting with an initial guess for pressure, film thickness and temperature. The generalized Reynolds, linear elasticity and load balance equations are solved simultaneously using a damped Newton procedure [26]. The resulting pressure and film thickness distributions are used as inputs to the solution of the thermal problem defined by equations (10-11) which are also solved simultaneously. An iterative procedure is thus established between the respective solutions of the EHL and thermal parts, and repeated until the pressure and temperature solutions are converged. Note that for highly loaded contacts, special stabilized finite element formulations are needed for the solution of the generalized Reynolds equation. Similar formulations are also needed for the solution of the energy equations in a

convection-dominated regime. For more details about numerical and computational/modeling aspects, the interested reader is referred to [16].

## 4. Results and Discussion

In the current work, steel-steel circular contacts under both pure-rolling and rolling-sliding conditions are considered under a wide range of operating conditions. The employed lubricant is Shell T9, which properties have been detailed earlier. The operating conditions and material properties are summarized in Table 1.

| Property | Value |
|---|---|
| Steel Young's Modulus | 210 GPa |
| Steel Poisson Coefficient | 0.3 |
| Steel thermal conductivity $k$ | 46 W/m.K |
| Steel heat capacity $c$ | 470 J/kg.K |
| Steel density $\rho$ | 7850 kg/m$^3$ |
| Sphere Radius $R$ | 12.7 mm |
| Lubricant inlet viscosity $\mu_0$ | 0.0135 Pa.s |
| Inlet reciprocal isoviscous pressure $\alpha^*$ | 20.25 GPa$^{-1}$ |
| Lubricant inlet thermal conductivity $k_0$ | 0.1114 W/m.K |
| Lubricant inlet heat capacity $c_0$ | 1337.14 J/kg.K |
| Inlet temperature $T_0$ | 25ºC |
| Reference temperature $T_R$ | 25ºC |
| External Applied Load $F$ | 5, 10, 20, 40, 80, 160 and 320 N |
| Hertzian contact pressure $p_h$ | 0.43, 0.54, 0.68, 0.86, 1.09, 1.37 and 1.72 GPa |
| Mean Entrainment Speed $U_m$ | 0.1 - 10 m/s |
| Slide-to-Roll Ratio $SRR$ | 0.0 - 0.25 |
| Range of Moes [27] dimensionless parameters | $5 < M < 10{,}000$ and $5 < L < 15$ |

**Table 1:** Operating conditions and lubricant and solid material properties

Note that for all load and speed conditions employed in this work, an adequate unstructured mesh has been employed in the numerical model so as to ensure that the reported solutions are grid-independent and avoid problems pertaining to the mesh sensitivity of EHL solutions under high loads [28]. The objectives of this section are: first, to quantify the importance of compressive heating/cooling in TEHL circular contacts as a function of the operating conditions and provide a quantitative comparison with shear heating, and second to quantify the impact of compressive heating/cooling on the lubrication performance of these contacts.

### 4.1. Compression vs. Shear Heating

First, the effects of external applied load and entrainment speed on compressive heating/cooling under pure-rolling conditions are examined. Figure 2 shows variations of $Q_{comp}$ with external applied load and entrainment speed in the mid-layer of the lubricant film along the central line of the contact in the $x$-direction. There are two clearly distinct regions: the inlet region of the contact where compressive heat generation occurs ($Q_{comp}>0$) and the exit region where decompressive heat removal/cooling occurs ($Q_{comp}<0$) except in the vicinity of the pressure spike (a localized heating region is observed). Looking at the corresponding pressure profiles in figure 3, it is clear that pressure rises in the inlet region while it decreases in the exit region except in the vicinity of the pressure spike (a localized pressure increase occurs).

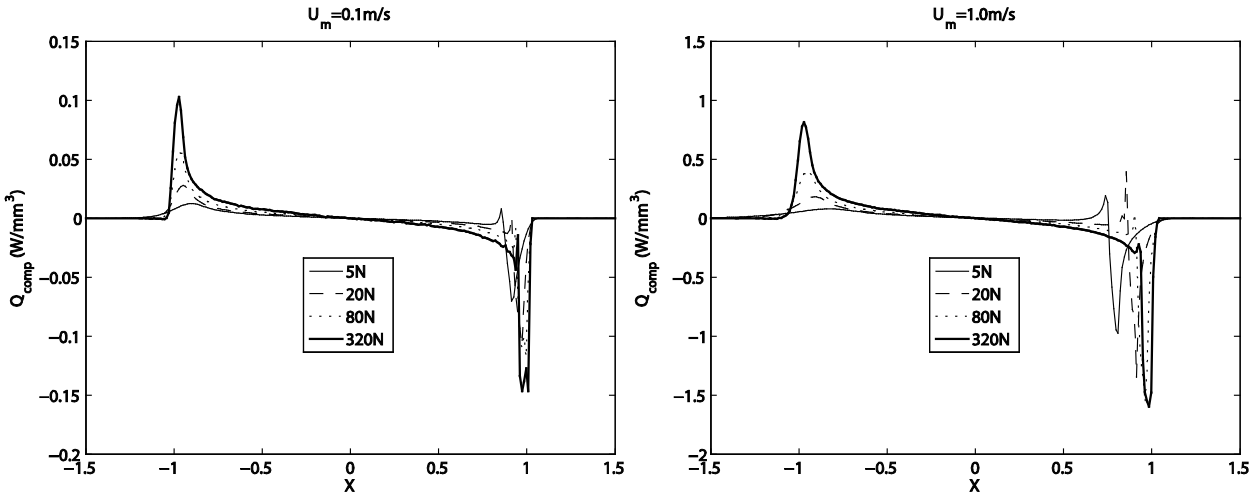


**Figure 2:** Variation of $Q_{comp}$ with load in the middle layer of the lubricant film along the central line of the contact in the *x*-direction under pure-rolling conditions (Left: $U_m$=0.1m/s; Right: $U_m$=1m/s)

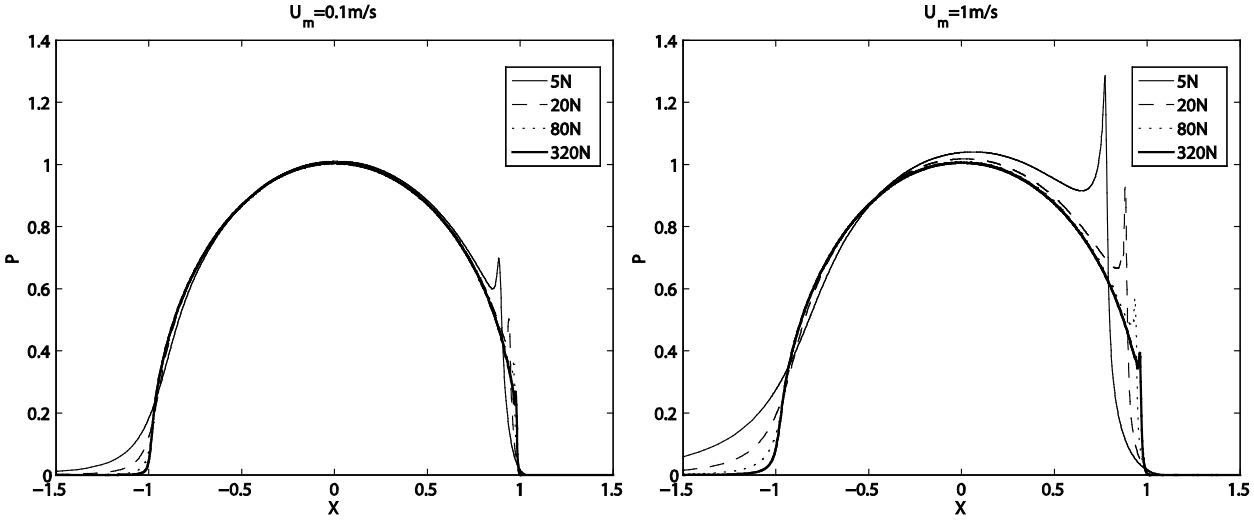


**Figure 3:** Variation of dimensionless pressure P with load along the central line of the contact in the *x*-direction under pure-rolling conditions (Left: $U_m$=0.1m/s; Right: $U_m$=1m/s)

It is clear from figure 2 that the magnitude of $Q_{comp}$ increases with both load and speed. Note that the scale in the right figure is ten times larger than in the left figure and that in terms of magnitude, 1W/mm$^3$ corresponds to a significant amount of volumetric power generation. This emphasizes the importance of considering power dissipation/losses in EHL conjunctions even under pure-rolling conditions. The increase with load is associated with the sharper pressure gradients observed in figure 3 in both the inlet and exit regions of the contact as the external applied load is increased. As for the increase with the mean entrainment speed, it is associated with the increase in the lubricant velocity within the lubricant film. In fact, a careful examination of the expression of $Q_{comp}$ in equation (11) (the bracketed terms in particular) reveals that it is proportional to both pressure gradients and the lubricant velocity within the contact. The increase in compressive heating/cooling with mean entrainment speed has also been reported in the experimental work of Reddyhoff et al. [14]. However, in their work, the effect of the external applied load was not examined and only one value was considered. Note also that the numerical

model employed in this work does not allow the consideration of the "nominally pure-rolling" conditions used by Reddyhoff et al. in which the ball is entrained by the disc and some sliding may not be prevented. Only the "pure-rolling" case is considered where both surface velocities are forced to be exactly the same.

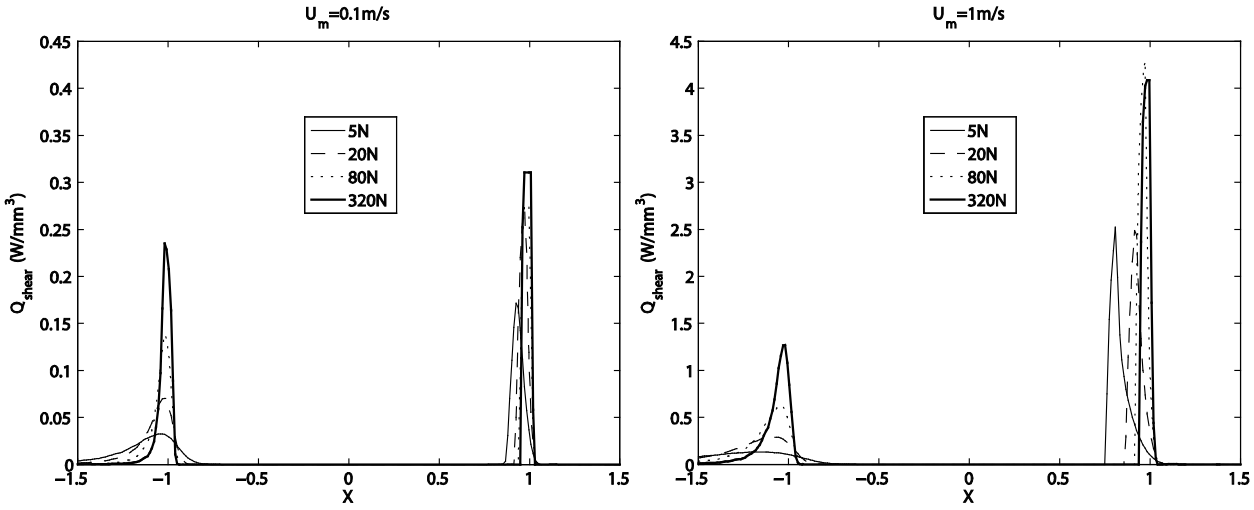


**Figure 4:** Variation of $Q_{shear}$ with load on the surface of the contacting solids along the central line of the contact in the *x*-direction under pure-rolling conditions (Left: $U_m$=0.1m/s; Right: $U_m$=1m/s)

Figure 4 shows the variations of $Q_{shear}$ with external applied load and entrainment speed in the mid-layer of the lubricant film along the central line of the contact in the *x*-direction under pure-rolling conditions. As with $Q_{comp}$, there are two distinct regions: the inlet region and the pressure spike region which experience relatively higher pressure gradients than the rest of the contact. The higher pressure gradients lead to higher shear rates associated with the corresponding "Poiseuille" flow and thus higher heat generation by shear. Note that in the central region of the contact, owing to the relatively lower pressure gradients, heat generation by shear is negligible, but this is only true under pure-rolling conditions. If sliding was to occur, owing to the relatively small film thickness in this area, shear heating corresponding to the "Couette" flow component would become much more important. Finally, by comparing the magnitudes of $Q_{comp}$ and $Q_{shear}$ in figures 2 and 4, it is clear that, contrarily to what is commonly believed, the latter is at least of the same order of magnitude or greater than the former even under pure-rolling conditions. This issue will be discussed in further details next.

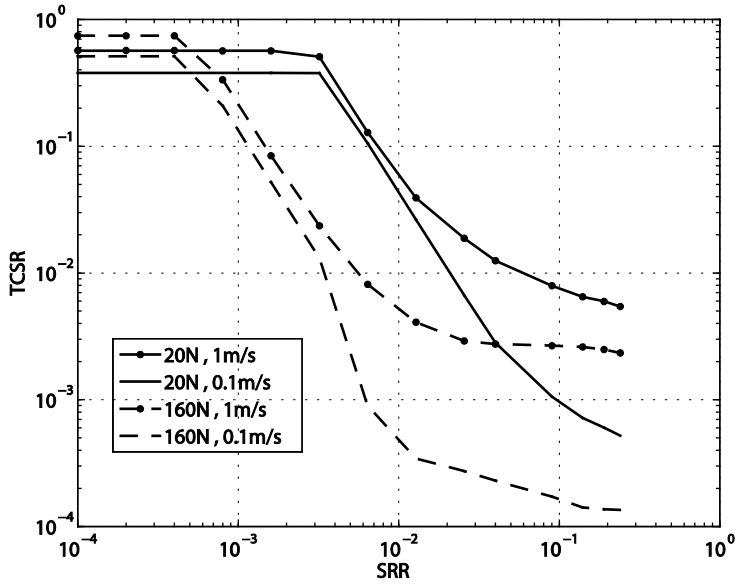


**Figure 5:** Thermal Compression-to-Shear Ratio (TCSR) as a function of Slide-to-Roll Ratio (SRR) under different load and speed conditions on a log-log scale

In fact, in order to quantify the importance of $Q_{comp}$ as compared to $Q_{shear}$, a new dimensionless number called "Thermal Compression-to-Shear Ratio" (*TCSR*) is defined as follows:

$$TCSR = \left.\frac{\max\left(Q_{comp}\right)}{\max\left(Q_{shear}\right)}\right|_{x<0} \qquad (13)$$

This dimensionless number represents the ratio of maximum heat generation by compression to that by shear in the region extending from the inlet of the contact to the central part (x<0). The choice to ignore the exit region of the contact (x>0) is based on the fact that the effect of compressive heating on the lubrication performance of the contact is restricted to the inlet region while very little effect is observed in the exit region as will be discussed in the following section. In addition, it is well-known in EHL that the exit of the contact has very little influence on its lubrication performance. As such, ignoring the exit region of the contact in the definition of TCSR is expected to have very little importance. It is also important to mention that this avoids dealing with the value of $Q_{shear}$ in the vicinity of the pressure spike, which is not very accurate as it is somehow related to the spike's height which in its turn is not accurately captured unless an extremely fine mesh is employed. But this would be a prohibitive price to pay in terms of computational cost given that compressive heating has very little effect in this region irrespective of the operating conditions as will be discussed later.

Figure 5 shows the variation of *TCSR* as a function of the Slide-to-Roll Ratio (*SRR*) under different load and mean entrainment speed conditions. Note that even at very low *SRR*, $TCSR \approx 1$ implying that both compressive and shear heating are of similar importance. This contradicts the common belief that under such conditions heat generation is dominated by compression. Also

note that any slight amount of sliding would lead to a drastic decrease in the value of *TCSR*. In fact, whenever SRR exceeds 0.003 (for the 20N/0.68GPa case) or even 0.0004 (for the 160N/1.37GPa case) the value of *TCSR* exhibits a drastic decrease. This being said, the "nominally-pure rolling" tests considered by Reddyhoff et al. [14] in their experiments (carried out at 0.97GPa) must entail a significant amount of shear heating as in these cases, sliding is virtually impossible to prevent entirely. Also note that with increasing load, not only does the dominance of shear heating start at lower SRR values, it also becomes more and more pronounced, but this effect decreases with mean entrainment speed. Finally, note that at high *SRR*, *TCSR* tends towards an asymptotic value. This is due to two factors: first; the limiting shear stress is reached at the center of the contact and with increasing *SRR*, the region where the limiting shear stress is reached extends to the entire hertzian contact region where most of the heat generation by shear occurs and second; shear heating in the central part of the contact is offset by a viscosity decrease in this region as a consequence of both shear-thinning and temperature increase. And since the magnitude of $Q_{comp}$ does not depend on *SRR*, a limiting value for *TCSR* is reached at high *SRR*.

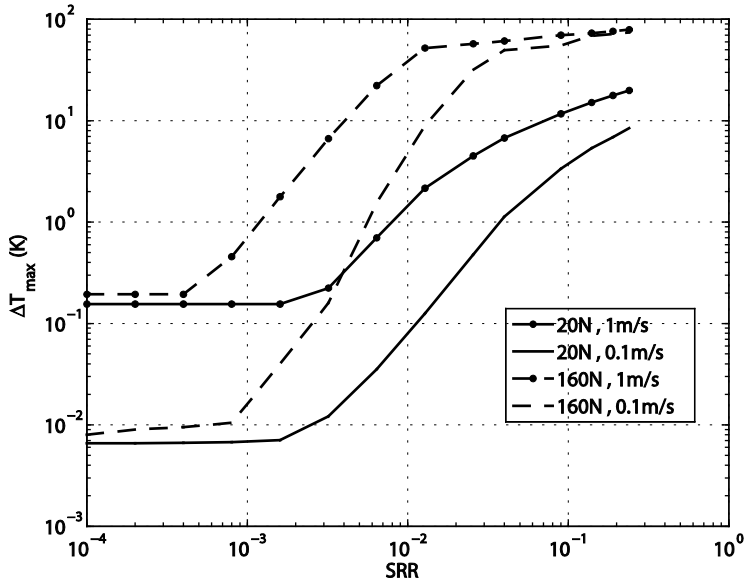


**Figure 6:** Maximum temperature increase within the lubricant film as a function of Slide-to-Roll Ratio under different load and speed conditions on a log-log scale

Figure 6 shows the maximum temperature increase within the lubricating films corresponding to the cases considered in Figure 5. It is clear that temperature increase within the lubricant film is somehow related to *TCSR*. One can see that the increase in temperature with *SRR* coincides with the decrease in *TCSR*. In other words, temperature starts significantly increasing only when shear heating becomes significant. Also, temperature increase with *SRR* reaches an asymptotic value for the same reasons as *TCSR*. Finally, note that temperature rise increases with load for a given speed and also increases with speed for a given load.

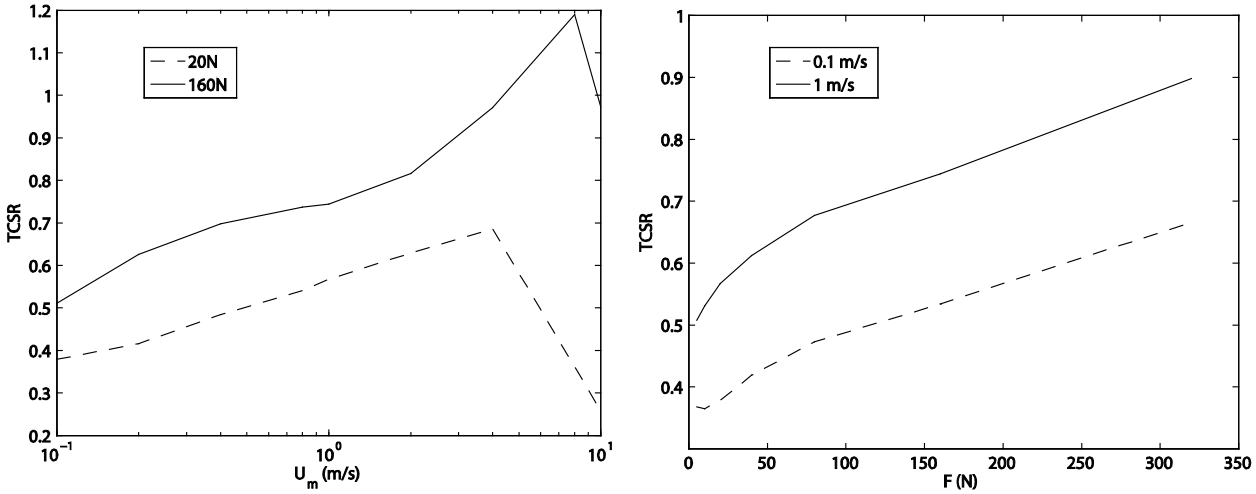


**Figure 7:** Thermal Compression-to-Shear Ratio (TCSR) as a function of mean entrainment speed (Left) and load (Right) under pure-rolling conditions

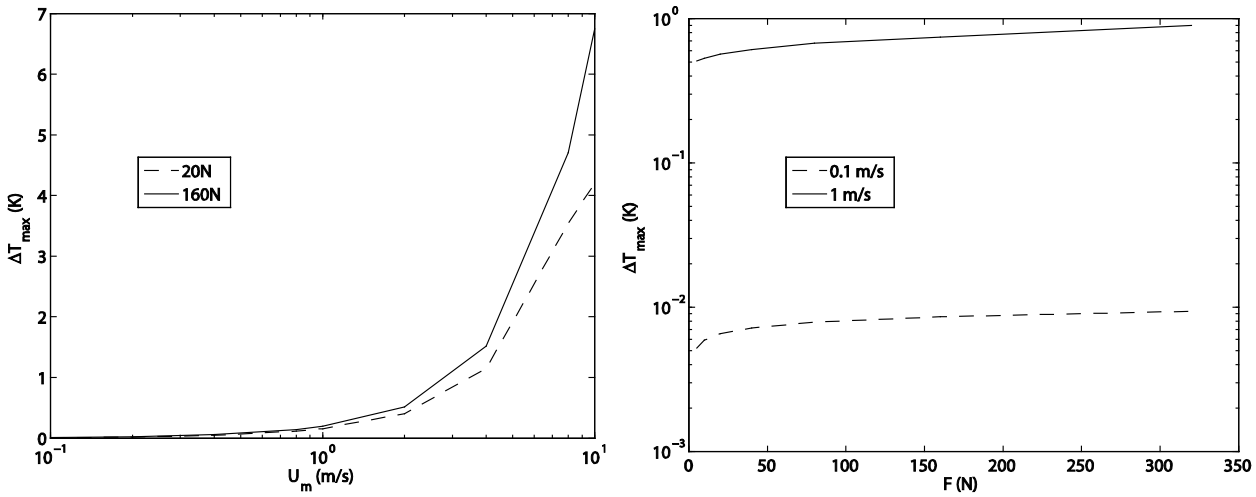


**Figure 8:** Maximum temperature increase within the lubricant film as a function of mean entrainment speed (Left) and load (Right) under pure-rolling conditions

Figure 7 shows the variations of *TCSR* with mean entrainment speed (left) and external applied load (right) under pure-rolling conditions. The corresponding maximum temperature rises are shown in figure 8. Note that, contrarily to common belief, even under pure-rolling conditions, compressive and shear heating are of the same order for the entire range of operating conditions considered here. Only under very high mean entrainment speeds does compressive heating slightly exceed shear heating but as can be seen in figure 7 (left), if speed is further increased this tendency is inverted and shear heating re-becomes more dominant. Regarding the dependence of *TCSR* on the external applied load, figure 7 (right) shows that it continuously increases with load at a given mean entrainment speed. As for temperature rise within the corresponding lubricant films, examining figure 8 it is clear that temperature rise with load is minimal. Yet, with increasing speed it becomes rather significant especially for mean entrainment speeds exceeding 3 to 4m/s. However, a significant share of the temperature rise is to be attributed to shear heating as suggested by the corresponding values of *TCSR* in figure 7.

Next, the effects of compressive heating on the lubrication performance of EHL contacts are examined.

### 4.2. Compressive Heating/Cooling Effect on Lubrication Performance

As indicated in the previous section, shear heating dominates heat generation in EHL contacts as soon as the slightest sliding occurs. Therefore, in this section, in order to focus on the effects of compressive heating on the lubrication performance of EHL contacts, only pure-rolling conditions are considered.

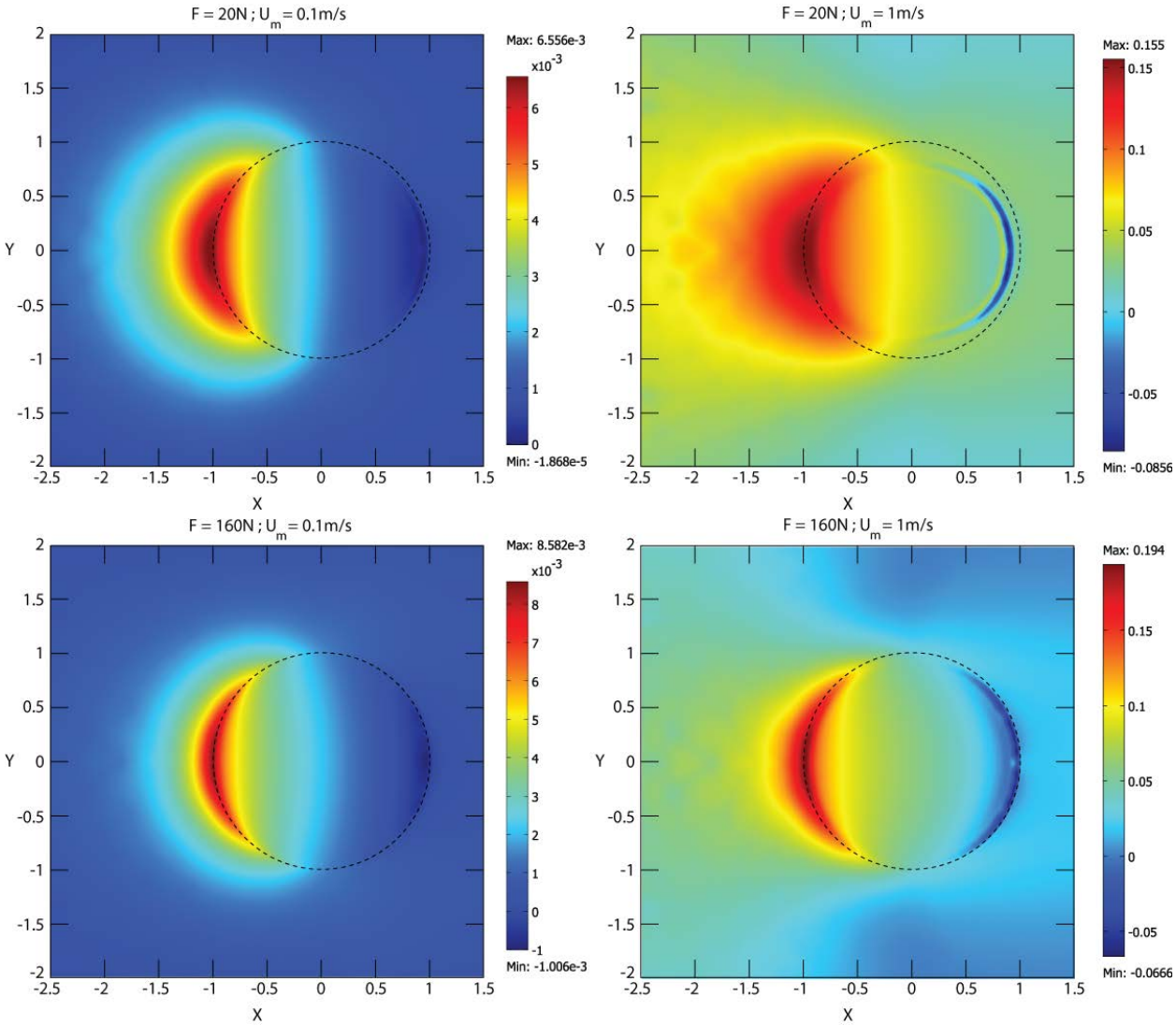


**Figure 9:** Temperature rise maps across the middle layer of the lubricant film under pure-rolling with different load (Top: 20N; Bottom: 160N) and mean entrainment speed (Left: 0.1m/s; Right: 1m/s) conditions

Figure 9 shows the temperature rise maps across the middle layer of the lubricant film under pure-rolling conditions for different external applied loads and mean entrainment speeds. The inlet of the contact is on the left side and the Hertzian contact region is delineated by a dashed circle. It is important to mention that these maps include the effects of compressive

heating/cooling as well as shear heating. As mentioned previously, the latter is at least of equal importance as the former. A careful examination of figure 9 suggests that, as noted earlier, temperature rise generally increases with both load and speed (though the increase with load is minimal as mentioned earlier). Note that with increasing load, temperature rise tends to be more focused in the central Hertzian region of the contact. This is a consequence of the pressure profile which tends towards a Hertzian pressure distribution as the external applied load is increased. Also note that with increasing speed, temperature rise tends to spread towards the inlet of the contact because of the extension of the pressure rise to that area (pressure distribution tends more towards a hydrodynamic profile rather than a Hertzian one) as well as the increased inlet shear heating. Decompressive cooling in the exit region of the contact also tends to become more pronounced owing to much larger pressure gradients associated with the presence of a sharper pressure spike. These results are globally of the same order of magnitude compared with the experiments of Reddyhoff et al. [14] carried out for a lubricant of similar properties. Finally, as expected, the maximum temperature rise occurs in the inlet at the edge of the Hertzian region while the lowest temperatures are observed on the opposite edge towards the exit. This is directly linked to the maximum values of both $Q_{comp}$ and $Q_{shear}$ in these regions as noted in figures 2 and 4 respectively.

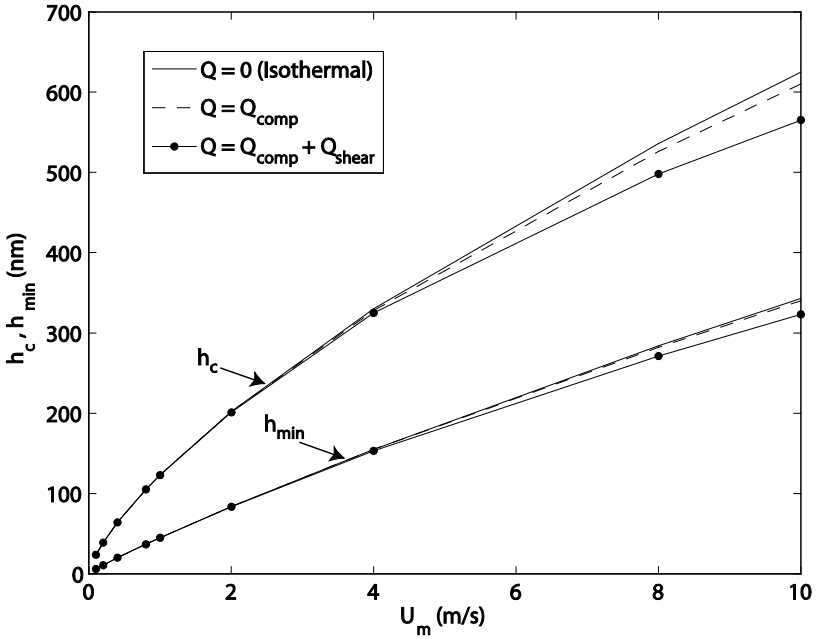


**Figure 10:** Effect of $Q_{comp}$ and $Q_{shear}$ on central and minimum film thickness as a function of mean entrainment speed under pure-rolling conditions and a constant external applied load of 160N ($p_h$=1.37GPa)

Finally, figure 10 shows the central ($h_c$) and minimum ($h_{min}$) film thickness variations with mean entrainment speed under pure-rolling conditions for an external applied load of 160N. The usual log-log representation is not employed here for better clarity. Only one load is considered in this test since the external applied load has been shown in figure 8 to have little effect on temperature rise within the lubricant film. In order to really isolate and quantify the effects of compressive heating on the lubrication performance, three separate cases are considered: an

isothermal case (solid lines) where both $Q_{comp}$ and $Q_{shear}$ are set to zero within the numerical simulations and two thermal cases where in the first only $Q_{comp}$ is considered while $Q_{shear}$ is set to zero (dashed lines) and in the second both $Q_{comp}$ and $Q_{shear}$ are considered (dotted solid lines). A careful examination of figure 10 reveals that under pure-rolling conditions, compressive heating/cooling has very little effect (if not none at all) on minimum film thickness and that any reduction in the latter at high mean entrainment speed is due to shear heating. This is why the definition of the dimensionless parameter *TCSR* introduced earlier was restricted to the part of the contact extending from the inlet region to the center. As for central film thickness, clearly both compressive and shear heating tend to decrease it but this is restricted to high mean entrainment speeds. This decrease is a consequence of a reduction in the lubricant's viscosity in the inlet region of the contact. The reduction in viscosity is associated with the rise in temperature in that region as noted in the temperature maps of figure 9. However, note that a significant part of the central film thickness reduction is due to shear heating. In fact, the sole contribution of compressive heating can be assessed by the deviation of the dashed line from the solid one. Therefore, it would be legitimate to say that the only configuration where compressive heating has any noticeable effect on the lubrication performance of EHL contacts is under pure-rolling conditions and high mean entrainment speeds and that this effect is restricted to central film thickness.

**Remark:** Friction curves were derived for the cases $Q=Q_{comp}$ and $Q=Q_{comp}+Q_{shear}$ with a mean entrainment speed of 1m/s and two external applied loads (20N and 160N) but the results are not shown here as no noticeable difference was observed between the cases where only compressive heating is considered and those where both compressive and shear heating are taken into consideration. This contradicts the findings of Kaneta et al. [11] who found that compressive heating has a significant influence on friction in EHL contacts. However, their results are somehow unusual and unexpected especially that in some cases, friction coefficients obtained with compressive heating only were lower than those obtained under the combined effects of compressive and shear heating.

## 5. Conclusion

This paper presents a numerical investigation of the compressive heating/cooling mechanism occurring within lubricating films in EHL contacts. It provides a quantitative evaluation of its importance as compared to shear heating under various normal loads and mean entrainment speeds with pure-rolling as well as rolling-sliding conditions. All numerical tests were carried out using a well characterized mineral oil. However, it is important to mention that the mechanism of compressive heating/cooling should not vary significantly from one lubricant to another, and as such, the findings of the current work may be regarded as being of a general validity.

It is found that even under pure-rolling, contrarily to what is commonly believed, compressive heating/cooling remains in most cases less important than shear heating or at best,

of the same order. However, under rolling-sliding conditions, as soon as the slightest sliding occurs, heat generation within these contacts is governed by shear heating. An important lesson to be extracted from this observation is that the use of “nominally pure-rolling” conditions to study compressive heating/cooling in TEHD contacts is inappropriate. Even a slight amount of sliding may have a significant impact on the thermal response of the contact.

The dependence of compressive heating/cooling on operating conditions is also examined under pure-rolling conditions. It is shown that the thermal compression-to-shear heating ratio (*TCSR*) exceeds unity only under very high mean entrainment speeds but when speed is further increased it eventually falls back below unity and shear heating re-becomes the dominant source of heat generation within the lubricant film. Also, *TCSR* was found to continuously increase with the external applied load for a given mean entrainment speed. Finally, the effects of compressive heating/cooling on the lubricating performance of EHL contacts was examined and it was concluded that the only configuration where compressive heating has any noticeable effect is under pure-rolling conditions and high mean entrainment speeds and that this effect is restricted to central film thickness. The latter actually reduces with increasing compressive heating.

**Nomenclature**

$\eta$ : Lubricant’s Generalized Newtonian viscosity
$\mu$ : Lubricant’s viscosity
$\mu_0$ : Lubricant’s ambient pressure viscosity
$\mu_g$ : Lubricant’s viscosity at the glass transition temperature $T_g$
$\rho$ : Lubricant’s density
$\rho_p$ : Plane’s density
$\rho_R$ : Lubricant’s density at reference state
$\rho_s$ : Sphere’s density
$\Lambda$ : Limiting stress-pressure coefficient
$\tau$ : Shear stress
$\tau_L$ : Limiting shear stress
$a$ : Hertzian contact radius
$c$ : Lubricant’s heat capacity
$c_p$ : Plane’s heat capacity
$c_s$ : Sphere’s heat capacity
$C$ : Lubricant’s volumetric heat capacity
$F$ : Contact external applied load
$G$ : Lubricant effective shear modulus
$h$ : Lubricant film thickness
$h_c$ : Lubricant central film thickness
$h_{min}$ : Lubricant minimum film thickness
$k$ : Lubricant’s thermal conductivity
$k_p$ : Plane’s thermal conductivity

$k_s$ : Sphere's thermal conductivity
$Q_{comp}$ : Compression heat generation term
$Q_{shear}$ : Shear heat generation term
$p$ : Pressure
$P$ : Dimensionless pressure ($=p/p_h$)
$p_h$ : Hertzian contact pressure
$p_0$ : Ambient pressure
$p_R$ : Reference pressure
$R$ : Sphere's radius
$SRR$ : Slide-to-Roll ratio $=(u_s-u_p)/u_m$
$T$ : Temperature
$T_0$ : Ambient temperature
$T_g$ : Lubricant glass transition temperature
$T_R$ : Reference temperature
$TCSR$ : Thermal compression-to-shear ratio
$U_m$ : Mean entrainment speed $=( u_s+u_p)/2$
$u_f$, $v_f$ : Lubricant's velocity components in the $x$ and $y$ directions
$u_p$ : Plane's surface velocity
$u_s$ : Sphere's surface velocity
$V$ : Volume
$V_R$ : Volume at reference state
$x, y, z$ : Space coordinates
$X, Y, Z$ : Dimensionless space coordinates ($X=x/a$; $Y=y/a$; $Z=z/a$ (solids) or $Z=Z/h$ (lubricant))

**Subscripts**

$s$ : Sphere
$p$ : Plane
$0$ : Ambient conditions state
$R$ : Reference state

**References**


[1] Gohar R. – Elastohydrodynamics, 2nd edition, Imperial College Press, London (2001).
[2] Cheng H. S. and Sternlicht B. - A Numerical Solution for the Pressure, Temperature and Film Thickness Between Two Infinitely Long, Lubricated Rolling and Sliding Cylinders, Under Heavy Loads, *ASME J. Basic. Eng.*, 1965, vol. 87, pp. 695-707.
[3] Cheng H. S. - A Refined Solution to the Thermal-Elastohydrodynamic Lubrication of Rolling and Sliding Cylinders. *ASLE Trans.*, 1965, vol. 8, pp. 397-410.
[4] Zhu D. and Wen S. - A Full Numerical Solution for the Thermo-Elastohydrodynamic problem in Elliptical Contacts, *ASME J. of Tribol.*, 1984, vol. 106, pp. 246-254.
[5] Kim K. H. and Sadeghi F. - Three-Dimensional Temperature Distribution in EHD Lubrication: Part I – Circular Contact, *ASME J. of Tribol.*, 1992, vol. 114, pp. 32-41.

[6] Guo F., Yang P. and Qu S. - On the Theory of Thermal Elastohydrodynamic Lubrication at High Slide-Roll Ratios – Circular Glass-Steel Contact Solution at Opposite Sliding. *ASME J. of Tribol.*, 2001, vol. 123, pp. 816-821.
[7] Kaneta M., Shigeta T. and Yang P. – Film Pressure Distributions in Point Contacts Predicted by Thermal EHL Analysis, *Tribology International*, 2006, vol. 39, pp. 812-819.
[8] Liu X., Jiang M., Yang P. and Kaneta M. - Non-Newtonian Thermal Analyses of Point EHL Contacts Using the Eyring Model, *ASME J. of Tribol.*, 2005, vol. 127, pp. 70-81.
[9] Kazama T., Ehret P. and Taylor C. M. – On the Effects of the Temperature Profile Approximation in the Thermal Newtonian Solutions of Elastohydrodynamic Line Contacts, *Proc. IMechE. J. Engnrng. Tribol.*, 2001, Part J., vol. 215, pp. 109-120.
[10] Salehizadeh H. and Saka N. – Thermal Non-Newtonian Elastohydrodynamic Lubrication of Rolling Line Contacts. *ASME J. of Tribol.*, 1991, vol. 113, pp. 481-491.
[11] Kaneta M., Shigeta T., and Yang P. – Effects of Compressive Heating on Traction Force and Film Thickness in Point EHL Contacts, *ASME J. of Tribol.*, 2005, vol. 127, pp. 435-442.
[12] Sadeghi F. and Sui P.C. – Thermal Elastohydrodynamic Lubrication of Rolling/Sliding Contacts, *ASME J. of Tribol.*, 1990, vol. 112, pp. 189-195.
[13] Kim H.K. and Sadeghi F. – Three-Dimensional Temperature Distribution in EHD Lubriucation: Part I-Circular Contact, *ASME J. of Tribol.*, 1992, vol. 114, pp. 32-41.
[14] Reddyhoff T., Spikes H. A. and Olver A. V. – Compression Heating and Cooling in Elastohydrodynamic contacts, *Tribology Letters*, 2009, vol. 36, pp. 69-80.
[15] Habchi W., Eyheramendy D., Bair S., Vergne P. and Morales-Espejel G. – Thermal Elastohydrodynamic Lubrication of Point Contacts Using a Newtonian/Generalized Newtonian Lubricant, *Tribology Letters*, 2008, vol. 30 (1), pp. 41-52.
[16] Habchi W., Eyheramendy D., Vergne P. and Morales-Espejel G. – Stabilized Fully-Coupled Finite Elements for Elastohydrodynamic Lubrication Problems, *Advances in Engineering Software*, 2012, vol. 46, pp. 4-18.
[17] Habchi W., Vergne P., Bair S., Andersson O., Eyheramendy D. and Morales-Espejel G. E. – Influence of Pressure and Temperature Dependence of Thermal Properties of a Lubricant on the Behavior of Circular TEHD Contacts, *Tribology International*, 2010, vol. 43, pp. 1842-1850.
[18] Murnaghan, F.D. -The Compressibility of Media under Extreme Pressures, *Proceedings of the National Academy of Sciences*, 1944, Vol. 30, p. 244-247.
[19] Bair S., Mary C., Bouscharain N. and Vergne P. - An Improved Yasutomi Correlation for Viscosity at High Pressure, *Proc. IMechE. J. Engnrng. Tribol.*, 2013, Part J, vol. 227 (9), pp. 1056-1060.
[20] Bair, S. - A Rough Shear Thinning Correction for EHD Film Thickness, *STLE Tribology Trans*., 2004, Vol. 47, N°3, p. 361-365.
[21] Habchi W., Vergne P., Fillot N., Bair S. and Morales-Espejel G. E. – A Numerical Investigation of Local Effects on the Global Behavior of TEHD Highly Loaded Circular Contacts, *Tribology International*, 2011, vol. 44, pp. 1987-1996.
[22] Vergne P. and Bair S. – Classical EHL versus Quantitative EHL: A Perspective Part I – Real Viscosity-Pressure Dependence and the Viscosity-Pressure Coefficient for Predicting Film Thickness, *Tribology Letters*, 2014, vol. 54, pp. 1-12.
[23] Yang, P., Wen, S. - A Generalized Reynolds Equation for Non-Newtonian Thermal Elastohydrodynamic Lubrication, *ASME J. Tribol.*, 1990, vol. 112, pp. 631-636.

[24] Hartinger M., Dumont M.-L., Ioannides S., Gosman D. and Spikes H. - CFD Modeling of a Thermal and Shear-Thinning Elastohydrodynamic Line Contact, *ASME J. of Tribol.*, 2008, vol. 139, 041503.
[25] Wu S. R. – A Penalty Formulation and Numerical Approximation of the Reynolds-Hertz Problem of Elastohydrodynamic Lubrication. *Int. J. Engnrng. Sci.*, 1986, vol. 24 (6), pp. 1001-1013.
[26] Deuflhard P. – Newton Methods for Nonlinear Problems, Affine Invariance and Adaptive Algorithms. *Springer*, Germany, 2004.
[27] Moes H. – Optimum Similarity Analysis with Applications to Elastohydrodynamic Lubrication. *Wear*, 1992, vol. 159, pp. 57-66.
[28] Venner, C.H. - EHL Flm Thickness Computations at Low Speeds: Risk of Artificial Trends as a Result of Poor Accuracy and Implications for Mixed Lubrication Modelling, *IMechE, J. of Eng. Trib.*, 2005, vol. 219, pp. 285-290.